An Investigation of the Microstructure in the Pest Oxide of a MoSi2- Based Composite

CHAPTER *in* CERAMIC ENGINEERING AND SCIENCE PROCEEDINGS · MARCH 2008

DOI: 10.1002/9780470294635.ch57

6 AUTHORS, INCLUDING:

Mats Halvarsson
Chalmers University of Technology

Kristina Hellström
Chalmers University of Technology

AN INVESTIGATION OF THE MICROSTRUCTURE IN THE PEST OXIDE OF A $MoSi_2$-BASED COMPOSITE

Jun Eu Tang, Mats Halvarsson and Anders Kvist
Dept. of Experimental Physics
Chalmers / Goteborg University
SE-412 96 Gothenburg
Sweden

Kristina Hansson and Jan-Erik Svensson
Dept. of Environmental Inorganic Chemistry
Chalmers / Goteborg University
SE-412 96 Gothenburg
Sweden

Robert Pompe
Swedish Ceramic Institute
Box 5403
SE-402 29 Gothenburg
Sweden

ABSTRACT

The pesting of $MoSi_2$ was investigated by performing detailed microanalysis on the pest oxide layer. The studied material was a $MoSi_2$-Mo_5Si_3-clay composite which had undergone pest-oxidation for 4000 hours at 450°C. Results from detailed SEM and TEM studies, including quantitative EDX analysis, on the various features in the pest oxide are presented. It was found that $MoSi_2$, as well as the Mo_5Si_3, transforms immediately into an oxide mixture of MoO_3 nano-crystals and amorphous SiO_2 with significant loss in molybdenum upon oxidation. With time, part of the oxide mixture cluster into lamellar MoO_3 aggregates. These aggregates disappear from the oxide after even longer times, leaving voids in the oxide structure. This allows even quicker depletion of MoO_3 from the oxide, leaving dark grey regions containing mostly SiO_2.

INTRODUCTION

Molybdenum disilicide ($MoSi_2$) is widely used in high temperature applications owing to its high melting point (2020°C) and excellent resistance towards oxidation at very high temperatures. In the 400–600°C temperature range, however, it appears that the material suffers a major breakdown in oxidation resistance. The ensuing catastrophic oxidation, termed 'pesting', results eventually in structural disintegration.

The phenomenon has been the subject of years of research [1-12], during which several theories have been proposed. In many of these theories, the role of molybdenum trioxide (MoO_3) is questioned. It has been discovered that at temperatures below 750°C [1] the oxidation of $MoSi_2$ leads to the formation of MoO_3 and SiO_2. The MoO_3 is suspected to be the cause of the failure of the oxide as it gives rise to stresses in the oxide layer. This can be due to the massive volume expansion, which can be as large as 10 – 20 times [2], associated with the transformation. It was even suggested that the blisters [3] forming around the MoO_3 due to its evaporation are also to blame.

Of particular interest to this study is a $MoSi_2$-Mo_5Si_3-clay composite that is produced for use as heating elements. The material is formed from a $MoSi_2$ and Mo_5Si_3-containing powder mixture and a customised clay binder. Recent studies [12] have revealed that this material pests between

400 and 500°C with the peak pesting rate occurring around 470°C. In those studies, the kinetics were investigated by examining the pest layers after different durations of exposure and tracking the mass changes using thermo-gravimetric analysis (TGA) methods.

In this report, the focus was on the detailed characterisation of the pest oxide layer found on the material after a 4000-hour exposure in laboratory air at 450°C. The aim was to identify the phases on the pest oxide and their origins by linking their presence to their respective compositions, locations, microstructures as well as the condition of the surrounding oxide (e.g. cracks and pores).

EXPERIMENTAL

The specimens were, as those studied by Hansson et al (2000) [12], 3 mm-diameter rods fabricated at Kanthal AB. The rods were made of KS1800 ($MoSi_2$ with small amounts of Mo_5Si_3 and customised clay binder) material that was extruded into the desired shape and then sintered in several stages. For this investigation, they were subjected to oxidation at a constant temperature of 450°C for 4000 hours in laboratory air.

Sections of the oxidised rods were embedded in resin, then sawed, polished and thinly coated with conductive material. The prepared specimens were analysed in the Camscan S4-80DV scanning electron microscope (SEM) outfitted with a Link eXL energy dispersive x-ray (EDX) system for chemical analyses.

Thin (250 µm) cross-sectional slices of the oxidised rods were cut, polished and ion-etched to electron transparency for investigation in the JEOL 2000 FX transmission electron microscope (TEM) equipped with a LINK AN 10 000 EDX system. In addition, bits of oxide were shaved and crushed to fine powder. A suspension comprising the powder particles was applied in tiny drops onto sputtered carbon films stretched out over 3 mm-diameter copper grids. The powder was also analysed using the Philips CM 200 FEG TEM.

RESULTS AND DISCUSSION

Overview of the microstructure in the un-oxidised bulk

Before examining the pest oxide, the un-oxidised bulk of the specimens were analysed in the SEM in backscattered-electron mode. Atomic number contrast and EDX point analyses in the bulk revealed a predominant $MoSi_2$ polycrystalline phase with dark amoeba-shaped islands of clay (containing Si, Al, O, Mg among others) accompanied by small regions of Mo_5Si_3 (bright phase) with the various regions in contact with one another. A rough estimate of the relative quantities of each type is given as follows: 2% Mo_5Si_3, 15% clay, with the remaining being $MoSi_2$.

Phase identification in the oxide

Method and overview: The oxide, as seen in Fig. 1a, was around 600 µm thick and split by deep radial cracks running almost the entire thickness of the oxide. It also appeared to contain numerous thin lateral cracks, larger radial cracks and pores distributed across various different regions.

The various regions outlined by backscattered-electron contrast were identified as one of the five types listed in Table I along with their respective elemental compositions determined using EDX analysis. Details of the five distinct region types are described below, complete with examples in SEM and TEM images of the pest oxide.

Fig. 1 (b through d) is a series of SEM images of the oxide taken at higher magnifications at zones b) close to the interface (oxide front) c) in the inner middle part and d) in the outermost reaches of the oxide. The five different types of regions are featured in these images.

Medium grey (MG) regions: The medium grey regions, which will also be described as the 'matrix' oxide, dominated most of the thick oxide layer (see Fig. 1b - d). This region type was

Table I A summary of the types of regions in the pest oxide.

Region types	Features	Composition
White (W)	Tiny aggregates or thin strips in the oxide	MoO_3
Light Grey (LG)	Small areas originating from the Mo_5Si_3 phase	Mo:Si:O = 1:1:5
Medium Grey (MG)	Dominant 'matrix' oxide originating from the $MoSi_2$ phase	Mo:Si:O = 1:3:9
Dark Grey (DG)	Darker Mo-depleted regions surrounding cracks, formed from the MG regions	Mo:Si:O = 1:10:20
Black (B)	Clay and voids	Customised clay

seen as the oxidation product of the $MoSi_2$ in the bulk. A number of points in these regions were subjected to EDX analysis and the result was consistently that of molybdenum and silicon oxide

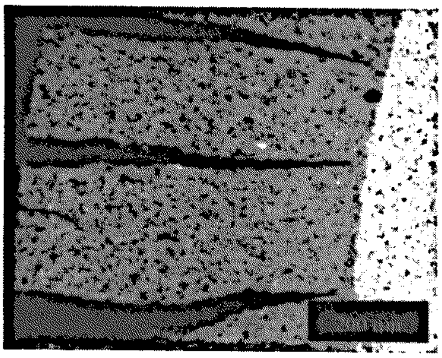

(a)

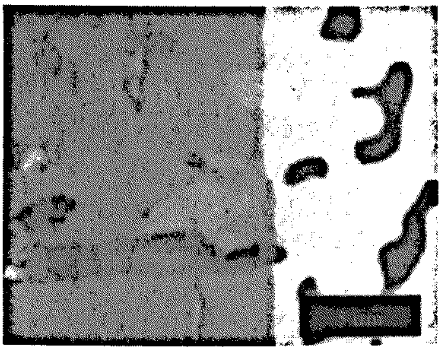

(b)

(c)

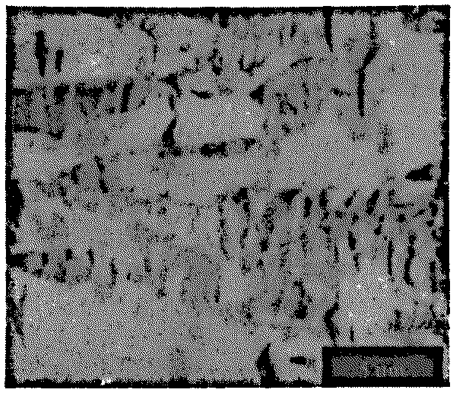

(d)

Fig 1 SEM backscattered-electron images featuring the (a) oxide overview (b) bulk-oxide interface (c) inner middle oxide (d) outermost oxide.

with a Mo:Si:O ratio of 1:3:9. The composition (compared to the Mo:Si ratio of 1:2 in bulk $MoSi_2$) reflected a drop in molybdenum concentration. It was found that the composition of this region type was relatively constant throughout the entire thickness of the oxide. As described earlier, bits of the oxide was finely crushed and the powder was subjected to TEM analysis. The oxide was analysed as small powder flakes. Fig. 2a is the bright field image of one such flake. The flake consisted of nanometre-sized particles dispersed in a matrix. Several locations on the flake were probed and the resulting EDX quantification showed that the compositions were constant and matched the analysis results obtained on the medium grey 'matrix' oxide in the SEM.

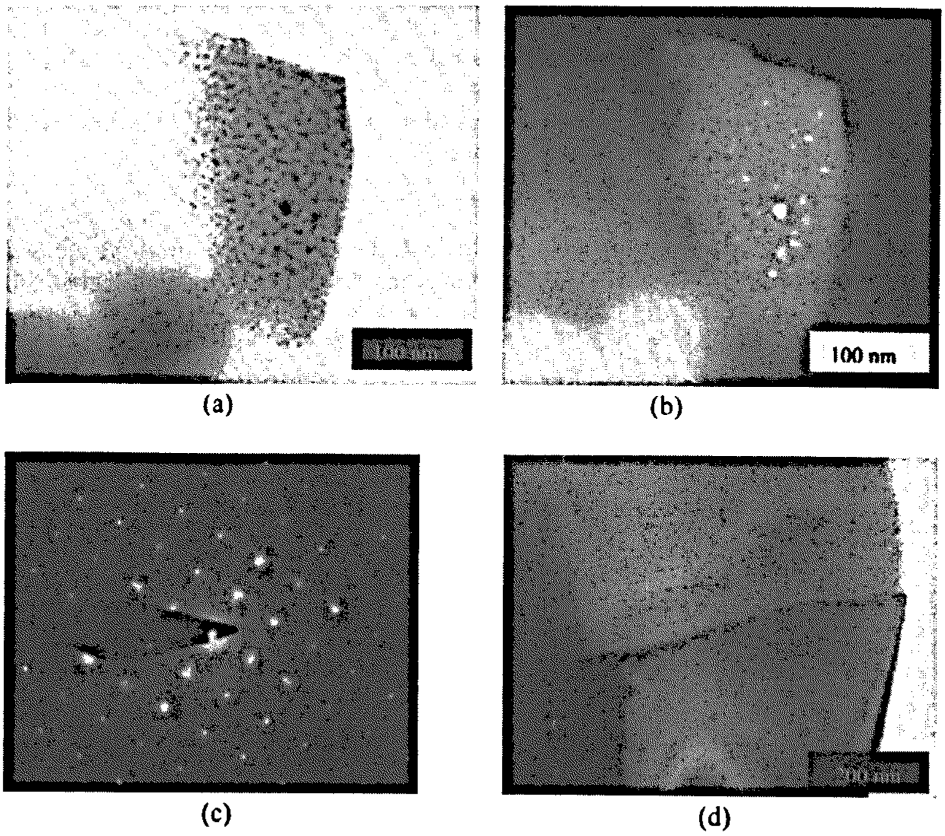

Fig. 2 (a) Bright and (b) dark field TEM images of a 'matrix' oxide flake. (c) Diffraction pattern of MoO_3 crystals. (d) TEM image of the bulk / oxide interface.

The nano-particles contained in the medium grey 'matrix' oxide flake were crystalline while the matrix was amorphous. Among the powder flakes, larger nano-particles were probed and EDX analysis yielded the composition MoO_3. Particle-free amorphous matrix flakes were also analysed and found to be SiO_2. Fig. 2b is the dark field image of the same powder flake where almost all the particles were bright which implied that they all had the same orientation relative to the incoming electron beam. This was an interesting observation, which suggested that the MoO_3 crystalline particles had an orientation relationship with the oxidation front. Diffraction patterns from some of the larger MoO_3 particles were recorded and indexed (Fig. 2c) to confirm that they were MoO_3 crystals exhibiting a tendency to lie with the (0 1 0) plane facing upwards on the grid. This observation was consistent with the results obtained in [4]. A cross-section TEM micrograph at the oxide interface is shown in Fig. 2d. On one side of the interface was a clear $MoSi_2$ grain, while the grainy molybdenum silicon oxide (MoO_3 nano-crystals in amorphous SiO_2 matrix) grain was right next to it. The oxide interface was clearly visible, confirming that $MoSi_2$ transforms upon oxidation into MoO_3 and SiO_2 while experiencing an almost immediate loss in molybdenum.

White (W) regions: The regions with the brightest contrast were referred to as the white regions. In Fig. 1b and 1c where they were present in large quantity, they took the form of tiny 'precipitates' or, more commonly, sets of near-parallel thin strips running in the lateral direction (parallel to the oxide interface). Such strips were not visible from the when the oxide area at 70 μm from the interface was viewed from the radial direction. This indicates that the strip-like white regions were sets of lamellae. EDX analysis of the thinner strips in the SEM was limited by the spatial resolution.

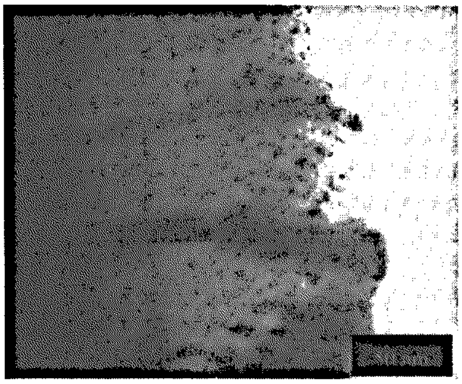

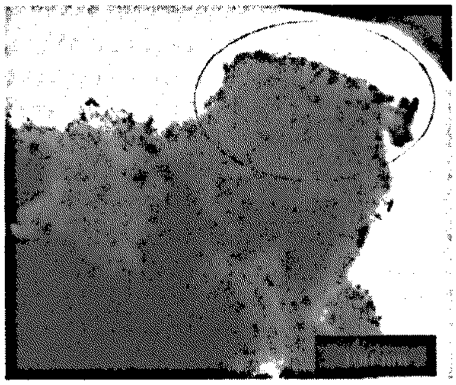

Fig. 3 TEM image of white MoO_3 strips. Fig. 4 Mo_5Si_3 (circled) region on a powder flake.

Similar thin strips were found in the cross-section TEM micrograph (see Fig. 3) of the pest oxide where EDX analysis and diffraction contrast proved that the strips were crystalline MoO_3. Using diffraction contrast in bright and dark field images, the tiny crystals in the strips were observed. While they did not all have the same orientation, a parallel-line pattern of similarly oriented crystals could be seen. This suggests an orientation relationship with the MoO_3 nano-crystals in the 'matrix' oxide as well as with the oxidation front although the exact relationship is still unknown at this point. It was speculated that these white MoO_3 regions were the result of segregation activity in the medium grey 'matrix' oxide. Many of the white strips were seen surrounded by small regions of darker (compared to the medium grey 'matrix' oxide) which were likely to be molybdenum-depleted.

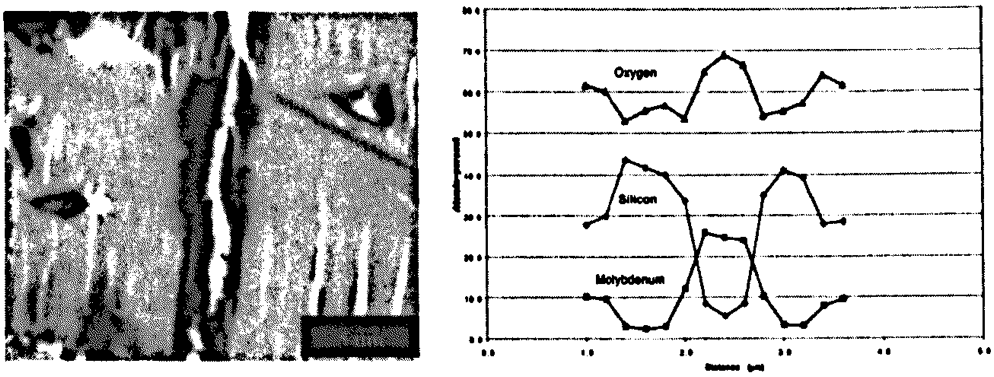

Fig. 5 A white strip surrounded by dark grey Mo-depleted region and the line-scan results showing mostly MoO_3 in the centre of the strip and mostly SiO_2 in the dark region.

While the majority of the strips were thin, there were a number of larger white strips surrounded by darker oxide regions.. One such strip (Fig. 5) was the subject of an EDX line scan including analysis points from within the white strip and the darker regions on both sides of it. The resulting molybdenum and silicon profiles showed a distinct peak in MoO_3 concentration (and a corresponding peak in oxygen level) in the white strip corresponding to a dip in silicon concentration. Another remarkable observation in this line scan was the depletion of molybdenum and corresponding enrichment in silicon in the immediate vicinity of the white strip, a clear sign of segregation activity.

Light Grey (LG) regions: These regions were of a light shade of grey and larger (to the order of 10 μm) than the white regions with a Mo:Si:O ratio of roughly 1:1:5. They were the post-oxidation Mo_5Si_3 regions. Fig. 1a shows a Mo_5Si_3 region stretching over from the bulk region into the oxide. This type of flake was also detected in the powder TEM samples, identified by comparing EDX results. Upon closer look (see Fig. 4), these regions were found to be similar in microstructure to the medium grey 'matrix' oxide regions in the sense that they also consisted of crystalline MoO_3 nano-particles in amorphous SiO_2 with a higher concentration of those particles.

Dark grey (DG) regions: The dark grey region type with low Mo content was also identified. They were most common in the outermost oxide (see Fig. 1d) and had Mo:Si:O ratios of around 1:10:20 (almost pure SiO_2). Such regions were also seen in the powder TEM samples.

Black (B) regions: As seen in Fig. 1b, the clay elongated after oxidation leaving large craters with dark stringy clay features across the region. The black regions represent such areas. Mainly SiO_2 was detected in those regions. The elongation suggested that the atoms of the clay phase might have been rearranged.

SEM analysis of the variation in the pest oxide

Method and overview: Obvious differences in the pest oxide microstructure at different distance from the interface were noted in the cross-section SEM image (See Fig. 1 b - d). Using the image analysis package available on the Link eXL EDX system, the relative abundance of three region types was tracked from the interface region outwards to the outermost oxide zone. Each measurement 'point' was a square area measuring 40 μm x 40 μm. The resulting depth profiles are presented in Fig. 6 where the relative abundance (in % of area analysed) was plotted against distance from the oxide interface with points in the oxide represented by the positive distances. The region types in the oxide were redefined into three types, such that the dark region included the dark grey (DG) (see Table I) and the black (B), the collective white region included the white (W) and light grey (LG) regions while the medium grey (MG) 'matrix' oxide remained as defined earlier. Two areas were analysed in the bulk and in those areas the bright region was Mo_5Si_3, the dark region was the clay binder and the grey region was the $MoSi_2$.

Bright regions: Bright regions are molybdenum-rich regions. In the oxide, where it represents the MoO_3 phase as well as the oxidised Mo_5Si_3, the level rose steadily to a maximum of 8 % at about 70 μm out in the oxide. After that, the level dropped until it reached a steady level of 2 % at 300 μm from the interface. This trend was confirmed by the observation that MoO_3 particles and lamellae were commonplace in the inner middle part (see Fig. 1c) of the oxide but had mostly vanished in the outer oxide (see Fig. 1d).

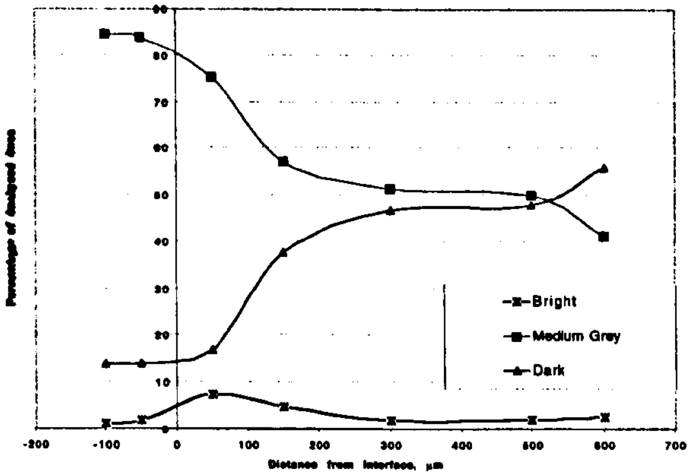

Fig. 6 Image analysis of different regions plotted against distance from the interface.

Dark regions: While there was a notable elongation (in the radial direction) of the clay regions as the oxide front crossed them, the area fraction remained constant until it began to rise at approximate 70 µm out in the oxide. Thereafter the level rose until it reached a steady level (48 %) in the areas between 300 and 500 µm from the interface after which it continued to rise in the outer oxide. The dark region also represents the molybdenum-depleted dark grey molybdenum silicon oxide regions that became common starting from the inner middle oxide zone and especially in the outermost oxide. In the middle of the oxide (see Fig. 1c), these regions were seen around white strips as well as around cracks and pores. In the outer oxide (see Fig. 1d), larger regions were found near cracks and pores.

Medium grey region: The profile appeared to be the opposite of the dark region profile, dropping to a steady level between 300 and 500 µm from the interface and then dropping further in a fashion almost complementary to that of the dark regions.

Discussion: The trend suggests that the initial oxidation was mostly a transformation of $MoSi_2$ together with the small amounts of Mo_5Si_3 into regions of crystalline MoO_3 and amorphous SiO_2. There appears to be a clustering of MoO_3 from the SiO_2 in parts of the oxide followed by the disappearance of the MoO_3 clusters leaving behind cracks and possibly giving rise to increased MoO_3-depletion from the oxide.

To find out if the overall composition showed any angular variation, area EDX analysis was performed at several positions in the oxide at the same distance from the oxide / bulk interface stretching from one radial crack to the next. The composition appeared not to have an angular dependence, thus returning the focus to depth dependence.

CONCLUSION

The pest oxide consists of complicated microstructure with five different types of regions. The dominant medium grey region, or 'matrix' oxide, is oxidised $MoSi_2$ which consists of MoO_3 nano-crystals and amorphous SiO_2. Mo:Si ratio is 1:3, which indicates that molybdenum is lost during oxidation. The nano-crystals appear to have the same orientation, indicating an orientation relationship with the oxidation front. A significant portion of the MoO_3 crystals soon clusters to form MoO_3 aggregates, present mostly as particulates or thin lamellae parallel to the oxide front in the 'matrix' oxide. These regions are present close to the oxide / bulk interface with a maximum at 70 µm from the interface. Beyond this zone, however, the white MoO_3 aggregates begin to disappear until, at more than 300 µm from the interface, they are virtually absent. Lateral cracks, which are present throughout the oxide, increase in numbers as the MoO_3 regions disappear. So do the dark grey regions, which are 'matrix' oxide regions from which MoO_3 is lost as MoO_3 clusters and as these clusters vanish, opening more voids. The molybdenum-depleted regions increase in volume fraction up to a level that is constant at between 300 and 500 μm from the interface, beyond which it increases further. Some of the 'matrix' oxide remains unaffected and retains its original composition. The black regions are clay remnants and pores, formed from the clay binder regions after oxidation. They undergo some atomic rearrangement as evidenced by the elongated craters (in the radial direction). Mo_5Si_3 oxidises into the light grey regions which consist of MoO_3 nano-crystals (more than in oxidised $MoSi_2$) and SiO_2. These regions likely experience the same MoO_3 loss as they are not seen in the outermost zone where the oxide is most aged. The above results are interpreted from the depth dependence of the microstructure. No angular dependence was observed.

REFERENCES

[1]C.D. Wirkus, and D.R. Wilder, "High-Temperature Oxidation of Molybdenum Disilicide," *Journal of the American Ceramic Society*, 49 173 (1966).

[2]C.G. McKamey, P.F. Tortorelli, J.H. DeVan, C.A. Carmichael, "A study of pest oxidation in polycrystalline $MoSi_2$", *Journal of Materials Research*, 7 [10] 2747-2755 (1992).

[3]T.C. Chou and T.G. Nieh, "Pesting of the High-Temperature Intermetallic $MoSi_2$," *JOM*, 15-21 (December 1993).

[4]R.W. Bartlett, J.W. McCamont and P.R. Gage, "Structure and Chemistry of Oxide Films Thermally Grown on Molybdenum Silicides," *Journal of the American Ceramic Society*, 48 551-558 (1965).

[5]E. Fitzer, "Oxidation of Molybdenum Disilicide"

[6]K. Yanagihara, K. Przybylski, T. Maruyama, "The Role of Microstructure on Pesting During Oxidation of $MoSi_2$ and $Mo(Si,Al)_2$ at 773 K," *Oxidation of metals*, 47 277-293 (1997).

[7]P.J. Meschter, "Low-Temperature Oxidation of Molybdenum Disilicide," *Metallurgical Transactions A*, 23A 1763 (1992).

[8]J.H. Westbrook and D.L. Wood, ""Pest" Degradation in Beryllides, Silicides. Aluminides, and Related Compounds," *Journal of Nuclear Materials*, 12 208-215 (1964).

[9]J.B. Berkowitz-Mattuck, P.E. Blackburn and E.J. Felten, "The Intermediate-Temperature Oxidation Behavior of Molybdenum Disilicide," *Transactions of the Metallurgical Society of AIME*, 233 1093-1099 (1965).

[10]H.J. Grabke and G.H. Meier, "Accelerated Oxidation, Internal Oxidation, Intergranular Oxidation, and Pesting of Intermetallic Compounds," *Oxidation of Metals an International Journal of the Science of Gas-Solid Reactions*, 44 147-176 (1995).

[11]J. Chen, C. Li, Z. Fu, X. Tu, M. Sundberg and R. Pompe, "Low Temperature Oxidation Behavior of a $MoSi_2$-Based Material," *Material Science and Engineering*, A261 239-244 (1999).

[12]K. Hansson, M. Halvarsson, J.E. Tang, J.-E. Svensson, M. Sundberg, R. Pompe, "On the Mechanism of $MoSi_2$ Pesting in the Temperature Range 400-500°C", *Proc. The 24th Annual Cocoa Beach Conference & Exposition, Cocoa Beach, Florida, USA, Jan 23-28, 2000, to be published.*